



**HAL**  
open science

## Analysis of the delayed damage model for three one-dimensional loading scenarii

Jihed Zghal, Nicolas Moes

► **To cite this version:**

Jihed Zghal, Nicolas Moes. Analysis of the delayed damage model for three one-dimensional loading scenarii. *Comptes Rendus. Physique*, 2021, 21 (6), pp.527-537. 10.5802/crphys.42 . hal-03140788

**HAL Id: hal-03140788**

**<https://hal.science/hal-03140788v1>**

Submitted on 27 May 2024

**HAL** is a multi-disciplinary open access archive for the deposit and dissemination of scientific research documents, whether they are published or not. The documents may come from teaching and research institutions in France or abroad, or from public or private research centers.

L'archive ouverte pluridisciplinaire **HAL**, est destinée au dépôt et à la diffusion de documents scientifiques de niveau recherche, publiés ou non, émanant des établissements d'enseignement et de recherche français ou étrangers, des laboratoires publics ou privés.



Distributed under a Creative Commons Attribution 4.0 International License



INSTITUT DE FRANCE  
Académie des sciences

# *Comptes Rendus*

---

## *Physique*

Jihed Zghal and Nicolas Moës

**Analysis of the delayed damage model for three one-dimensional loading scenarii**

Volume 21, issue 6 (2020), p. 527-537

Published online: 14 January 2021

Issue date: 14 January 2021

<https://doi.org/10.5802/crphys.42>

**Part of Special Issue:** Prizes of the French Academy of Sciences 2019 (continued)



This article is licensed under the  
CREATIVE COMMONS ATTRIBUTION 4.0 INTERNATIONAL LICENSE.  
<http://creativecommons.org/licenses/by/4.0/>



*Les Comptes Rendus. Physique sont membres du*  
*Centre Mersenne pour l'édition scientifique ouverte*  
[www.centre-mersenne.org](http://www.centre-mersenne.org)  
e-ISSN : 1878-1535



---

Prizes of the French Academy of Sciences 2019 (continued) / *Prix 2019 de l'Académie des sciences (suite)*

# Analysis of the delayed damage model for three one-dimensional loading scenarios

## *Analyse du modèle d'endommagement à effet retard pour trois scénarii de chargement mono-dimensionnel*

Jihed Zghal<sup>a</sup> and Nicolas Moës<sup>\*, b, c</sup>

<sup>a</sup> Laboratoire Energetique Mecanique Electromagnetisme (LEME), University of Paris Nanterre, 50 rue de sèvres 92410 Ville d'Avray, France

<sup>b</sup> Ecole Centrale de Nantes, GeM Institute, UMR CNRS 6183, 1 rue de la Noë, 44321 Nantes, France

<sup>c</sup> Institut Universitaire de France (IUF), France

*E-mails:* jzghal@parisnanterre.fr (J. Zghal), nicolas.moes@ec-nantes.fr (N. Moës)

**Abstract.** The delayed damage model has been introduced by Allix and Deü [1] as a way to overcome spurious mesh dependency in failure analysis involving damage and dynamic loading. The damage rate is bounded through a time scale which, combined with the wave speed, introduces implicitly a length scale. In this paper, the delayed damage model is analyzed through numerical experiments on three different loading cases of a bar: a slow loading leading to a dynamic failure, pulses and impact. We observe and discuss the load level needed for failure (and the dependence of this load level with respect to the loading rate), as well as the dissipation and extent of the fully damaged zone at failure. Observations lead to the following conclusions. First, the delayed damage model has no regularization effect for a dynamic failure initiating from rest. Second, for pulse loadings, the loading rate has no influence on the minimal load level needed for failure (even though the delayed damage model is a time-dependent model), and beyond this minimal load level for failure, the extent of the fully damage zone rises, proportionally to the length scale. Third, regarding the impact, the velocity needed to reach failure depends only the time-independent parameters of the models, and not the ones linked to the delayed damage.

**Résumé.** Le modèle d'endommagement à effet retard a été introduit par Allix et Deü [1] pour surmonter dans le cas de chargement dynamique la dépendance de maillage non-physique observée dans l'analyse de rupture. Le taux d'endommagement est limité via un temps caractéristique qui, combiné à la vitesse des ondes, introduit implicitement une longueur caractéristique. Dans cet article, le modèle d'endommagement à effet retard est analysé par des simulations numériques sur trois cas de chargement différents d'une barre : un chargement lent conduisant à une rupture dynamique, des impulsions et un impact. Nous observons et discutons le niveau de charge nécessaire à la rupture (et la dépendance de ce niveau de charge à la vitesse du chargement), ainsi que la dissipation et l'étendue de la zone entièrement endommagée lors de la rupture. Les observations conduisent aux conclusions suivantes. Premièrement, le modèle à effet retard n'a aucun effet de

---

\* Corresponding author.

régularisation pour une défaillance dynamique démarrant du repos. Deuxièmement, pour les chargements par impulsions, la vitesse de chargement n'a aucune influence sur le niveau de charge minimal nécessaire à la rupture (alors que le modèle à effet retard est pourtant un modèle dépendant du temps), et au-delà de ce niveau de charge minimal pour la rupture, l'étendue du dommage total est proportionnelle à la longueur caractéristique. Troisièmement, en ce qui concerne l'impact, la vitesse nécessaire pour atteindre la rupture dépend uniquement des paramètres affectant la version indépendante du modèle (et non ceux liés à l'effet retard).

**Keywords.** Damage, Delay effect, Dynamics, Localization, Softening.

**Mots-clés.** Endommagement, Effet retard, Dynamique, Localisation, Adoucissement.

## 1. Introduction

Damage growth simulation up to failure presents many challenges among which the need to introduce a length scale in the material model to avoid spurious mesh dependency even in the case of dynamic loading. This was observed already in [2] and further analyzed in [3] based on a viscoplastic model with void growth. If the length is absent, a single layer of elements may be affected by the damage localization. The level of dissipation to reach failure is then completely linked to the mesh size and not a physical parameter.

The length scale may be introduced directly in an explicit manner in the model. We find different types of approaches in this category as the non-local approach [4, 5] in which the damage growth at a point depends on the average of some quantity at some distance around the point. Kinematically based higher order gradient models [6, 7] develop a higher order kinematics (and equilibrium) introducing a length scale. Gradient based damage models [8–10] are yet other ways to introduce a length scale. The free energy depends both on damage and its gradient. One can also mention, more recent works as the phase-field approach emanating from the physics community [11], the variational approach to fracture [12] and the thick level set approach [13].

Another way to introduce a length scale in problems involving inertia effect is to rely on a time scale. This time scale multiplied by the wave speed introduces implicitly a length scale in the model. The time scale is usually introduced through a rate dependent model as in the early work by Needleman and co-workers [14] for plasticity and void growth. A comprehensive study may be found in the study [15]. Regarding damage, time-dependent version, may be traced back to [16], with further progress and application to concrete in [17]. These models are inspired from Perzyna plasticity [18].

Other rate dependent damage models have been proposed later to alleviate spurious localization as the delayed damage model which is the main focus of the paper. It was introduced in [1, 19]. The main difference between the previous form of rate dependency is that the delayed damage model bounds the damage rate to a material data parameter. Rate-dependent model are appealing from the computational point of view since they only affect the local constitutive stress update.

The goal of this paper is to test the robustness of the delayed damage model in specific scenarii. The first scenario is the sudden rupture of a pre-loaded bar. This scenario is interesting because the rupture is dynamical (unloading stress wave emanating from the rupture zone) while there is no initial kinetic energy in the bar. The second scenario, already considered in [2], deals with a bar loaded suddenly at both extremities. As the loading waves (pulses) reach the middle of the bar, they provoke rupture. Note that the loading is set so that damage can only start when both loadings superpose. The third scenario, considered first in [20], deals with the impact at the extremity of the bar: a sudden pulling velocity is applied. As in the first scenario, kinetic energy is

not initially present. Finally, even though the paper is dedicated to the delayed damage model, we will also discuss other formats for the introduction of the rate dependency as in [16] and [17].

We now detail the content of the paper. The next section gives the salient characteristics of the delayed damage model. The next three sections deal with one after the other the three scenarios, starting with the sudden rupture of pre-loaded bar, followed by the bar subjected to symmetrical tension pulses, and, finally, the impact scenario. Section 5 gives conclusions and discusses the expected results with other types of rate dependent damage models.

## 2. Delayed damage model for dynamics

The delayed damage model introduces a time scale denoted  $\tau_c$  [1, 19]. The main equation of the model is given by (1). It relates the damage rate  $\dot{D}$  to the energy release rate  $Y$ :

$$\begin{cases} \dot{D} = \frac{1}{\tau_c}(1 - \exp(-a\langle f(Y, D) \rangle_+)) & \text{if } D < 1 \\ D = 1 & \text{otherwise} \end{cases} \quad (1)$$

where  $a$  is a coefficient,  $\langle x \rangle_+ = (x + |x|)/2$  and the criteria  $f$  is given by:

$$f(Y, D) = \frac{\sqrt{Y} - \sqrt{Y_0}}{\sqrt{Y_c}} - D. \quad (2)$$

The value of  $Y$  for which damage starts is denoted by  $Y_0$ . The second parameter,  $Y_c$ , governs the damage hardening. It is clear from (1) that the damage rate is bounded by  $1/\tau_c$ . Multiplied by the wave speed  $c$ , the time scale brings a length scale  $l_c$ :

$$l_c = c\tau_c, \quad c = \sqrt{E/\rho} \quad (3)$$

where  $E$  is the Young modulus and  $\rho$  the density. In this paper, we will be considering one-dimensional models. The stress,  $\sigma$  is related to the strain  $\epsilon$  by the elasticity relation:

$$\sigma = E(1 - D)\epsilon \quad (4)$$

and the energy release rate is defined by:

$$Y = \frac{1}{2}E\epsilon^2. \quad (5)$$

Equations (1)–(2), (4)–(5) fully define the delayed-damage material model. For different imposed strain rates, Figure 1 shows the stress–strain relation, in which stress and strain have been normalized by their values when damage initiates:

$$\sigma_0 = \sqrt{2Y_0E}, \quad \epsilon_0 = \sqrt{2Y_0E^{-1}}. \quad (6)$$

## 3. First scenario: sudden rupture of a bar from rest

We now challenge the delayed damage model in the transition from a quasi-static to a dynamical situation. We consider a bar of length  $L$  and section  $S$  initially at rest and loaded in a quasi-static (ie infinitely slowly) manner to its limit point (top point on the quasi-static stress–strain curve, Figure 1). Because of the quasi-static nature of the loading, the bar reaches the limit point without any kinetic energy. Quantities at the limit point are denoted with the  $i$ . They may be obtained analytically:

$$D_i = \frac{\epsilon_c - \epsilon_0}{2\epsilon_c}, \quad \epsilon_i = \frac{\epsilon_c + \epsilon_0}{2}, \quad \sigma_i = (1 - D_i)E\epsilon_i \quad (7)$$

where  $\epsilon_c = \sqrt{(2Y_c/E)}$ .

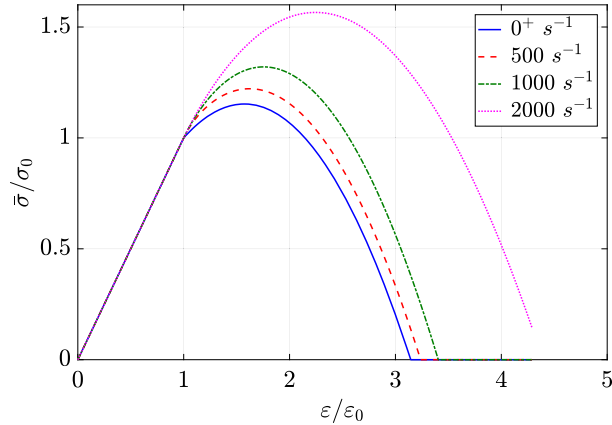


**Figure 1.** Stress vs strain for the delayed damage model considering different strain rates. The case  $0^+$  corresponds to a quasi-static loading.

**Table 1.** Material and geometrical properties properties (identical to those used in [1])

$E$ (MPa)	$\rho$ (kg/m <sup>3</sup> )	$Y_c$ (MPa)	$Y_0$ (MPa)	$a$	$\tau_c$ (s)	$L$ (m)	$S$ (m <sup>2</sup> )
$5.7 \times 10^4$	2280	0.23	0.05	10	$2 \times 10^{-6}$	0.1	$10^{-6}$

When the limit point has been reached, the loading is stopped and a small extra damage (related to  $\eta$  below) is applied at  $x = 0$ . The bar enters a dynamical regime towards rupture. Initial and boundary conditions for the displacement  $u$  are given by:

$$u(x, t = 0) = \epsilon_i x, \quad \dot{u}(x, t = 0) = 0, \quad D(x, t = 0) = \begin{cases} D_i, & x > 0 \\ (1 + \eta)D_i, & x = 0 \end{cases} \quad (8)$$

$$u(x = 0, t) = 0, \quad u(x = L, t) = \epsilon_i L. \quad (9)$$

The dynamic regime is governed by the linear momentum balance and strain compatibility:

$$\frac{\partial \sigma}{\partial x} = \rho \ddot{u}, \quad \epsilon = \frac{\partial u}{\partial x}. \quad (10)$$

The solution is sought over a time interval denoted  $T$ . The numerical values used for the simulations throughout the paper are given by Table 1.

Simulations are carried out using a classical explicit dynamic scheme [21]. In practice,  $\eta$  is taken at 0.01 and applied to the first element. Even though the loading does not evolve, the string is lead to catastrophic failure. During the simulation, we observe that damage grows only on the first element and faster as it reaches  $D = 1$ . The size of the zone which has reached  $D = 1$ , denoted  $l_1$ , and called failure length is thus restricted to a single element. This may be observed in Figure 2 giving the evolution of  $l_1$  with the mesh size. Regarding the dissipated energy

$$W_d = S \int_T \int_L Y \dot{D} dx dt \quad (11)$$

it is shown in Figure 3. The fact that it does not stabilize with the mesh size is a clear sign of spurious localization. Indeed, as the mesh size goes to zero, no energy is lost in the bar rupture. So, the fact that a minimal time is needed to reach  $D = 1$  in the model does not preclude spatial spurious localization in this example.

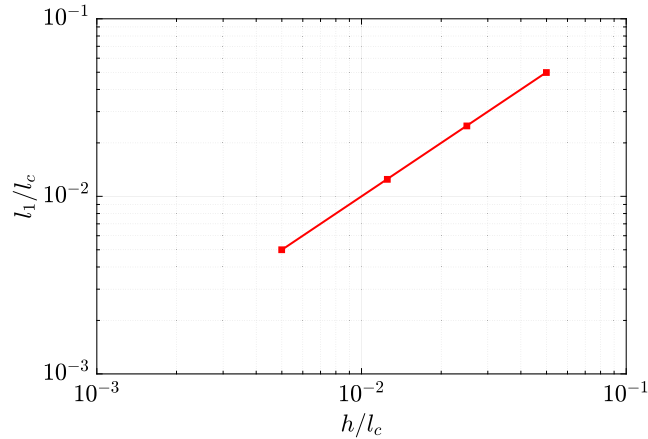


**Figure 2.** Failure length as a function of mesh size for the string problem.

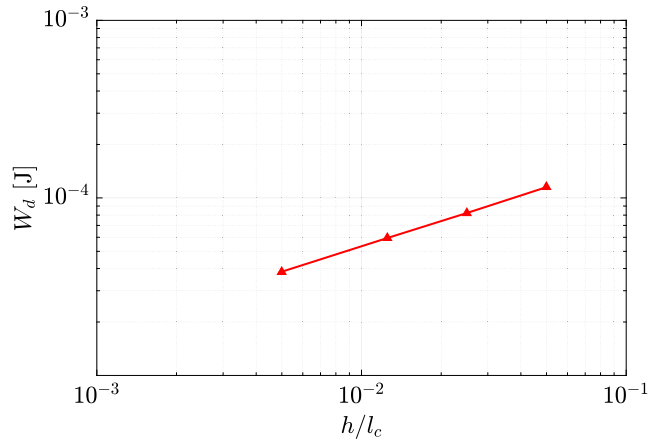


**Figure 3.** Evolution of the dissipated energy as a function of mesh size.

#### 4. Second scenario: a bar subjected to a sudden loading at both extremities

This scenario was already considered in [2]. Due to symmetry only half of the bar is considered (Figure 4). Initial and boundary conditions are

$$u(x, t = 0) = 0, \quad \dot{u}(x, t = 0) = 0, \quad D(x, t = 0) = 0 \tag{12}$$

$$u(x = 0, t) = 0, \quad \sigma(x = L/2, t) = \bar{\sigma}(t). \tag{13}$$

The loading evolution is given by:

$$\bar{\sigma}(t) = \min\left(\frac{E\dot{\epsilon}t}{2}, \frac{\bar{\Sigma}}{2}\right) \tag{14}$$

where  $\dot{\epsilon}$  is the loading rate affecting the duration,  $t_l = \bar{\Sigma}/(E\dot{\epsilon})$ , of the initial slope. We consider the loading to be small enough such that damage may only start when reflection occurs.

To analyze the damage pattern, as for the first scenario, we use the failure length concept introduced in [22] and denoted  $l_1$ . It corresponds at the end of the simulation to the size of the zone over which the damage has reached 1. We analyze numerically the relation between  $l_1$ , the

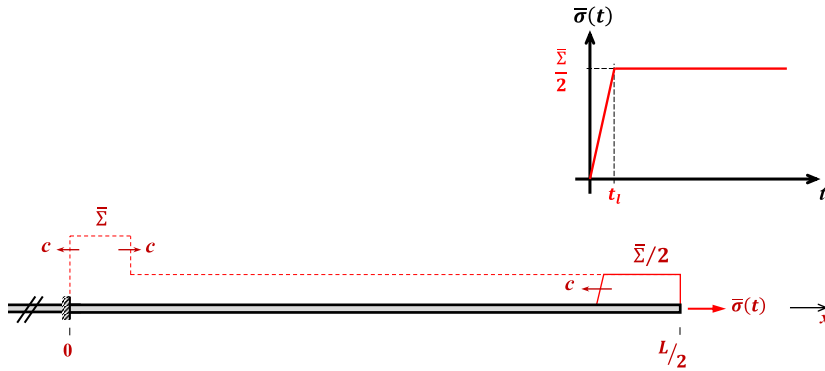


Figure 4. Bar under a pulse loading.

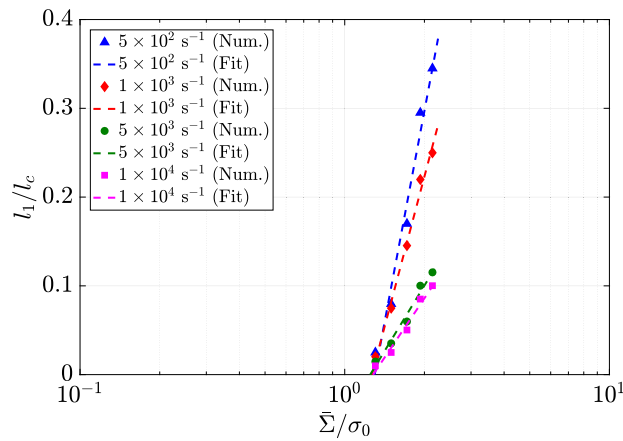


Figure 5. Failure length  $l_1$  as a function of the applied stress  $\bar{\Sigma}$  for different strain rates. Dashed lines correspond to a linear fit of the data.

applied load,  $\bar{\Sigma}$ , and the strain rate,  $\dot{\epsilon}$ . A linear relation between  $l_1$  and the log of the stress is observed in Figure 5 and summarized below:

$$l_1/l_c \sim \alpha(\dot{\epsilon}) \log \left( \max \left( \frac{\bar{\Sigma}}{\sigma_{loc}}, 1 \right) \right). \tag{15}$$

For the same final applied stress, the failure length tends to decrease when the loading rate increases. We also observe that the failure length collapses to zero for a given stress independently of the strain rate. We denote this stress as  $\sigma_{loc}$  and call it localization stress. It is the minimal stress needed to break the bar. It is observed numerically that  $\sigma_{loc}/\sigma_0 = 1.3$  for the material parameter given in Table 1.

When the loading is in between  $\sigma_{loc}$  and  $\sigma_0$ , damage develops but not enough to reach  $D = 1$ , so  $l_1 = 0$ . If the loading is below  $\sigma_0$ , damage does not develop at all. These regimes are illustrated in Figure 6 and summarized below.

$$\left\{ \begin{array}{ll} 0 < \bar{\Sigma} < \sigma_0 & \text{No Damage: } D = 0 \\ \sigma_0 \leq \bar{\Sigma} < \sigma_{loc} & \text{Damage but no failure: } 0 \leq D < 1 \\ \bar{\Sigma} = \sigma_{loc} & \text{Damage and failure: } D = 1 \text{ and } l_1 \rightarrow 0 \\ \bar{\Sigma} > \sigma_{loc} & \text{Damage and failure: } D = 1 \text{ and } l_1 > 0 \end{array} \right.$$

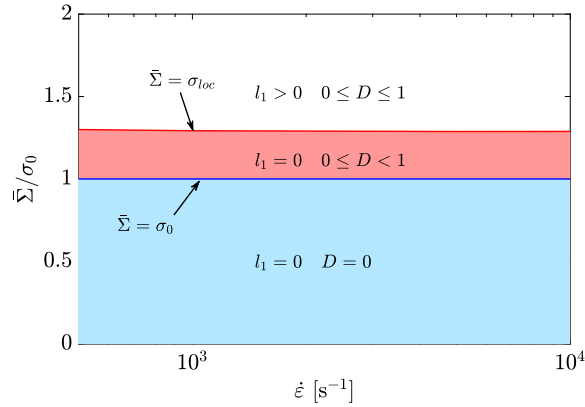


**Figure 6.** Three regimes depending on the stress level but independent of the loading rate.

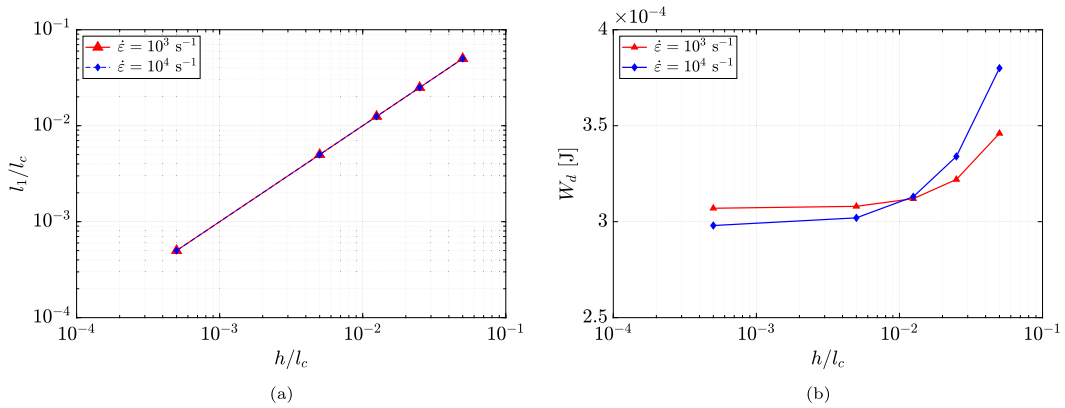


**Figure 7.** Failure length (a) as a function of mesh size and dissipated energy (b) when the localization stress is applied.

Note that a logarithmic relation between  $l_1$  and the applied stress was already given in [22, 23] but the dependence of  $l_1$  on the strain rate was not studied and the case where  $l_1$  was possibly zero was also not studied.

Figure 7(a) confirms that when the localization stress is applied, only a single element reaches  $D = 1$ , ( $l_1 = h$ ). Should we be worried by the fact that the failure length in the delayed damage may be limited to a single element? To answer this question, we analyze the energy dissipated. Figure 7(b) depicts the evolution of the dissipated energy with the mesh size. It seems to stabilize with the mesh size. We also analyze in Figure 8 the energy dissipated in the hardening and softening regions, respectively. At any given time, the hardening region is defined as the set of material points for which damage is not growing, or growing under a rising stress. The complementary part is the softening region, corresponding to a damage growth under diminishing stress.

$$W_d = W_d^{\text{hard}} + W_d^{\text{soft}}. \tag{16}$$

Both hardening  $W_d^{\text{hard}}$  and softening  $W_d^{\text{soft}}$  dissipated energy do stabilize with respect to the mesh size. So, on the contrary to the first scenario, for which the dissipation dropped constantly with the mesh size, dissipation stabilizes with the mesh size in the second scenario. The stabilization

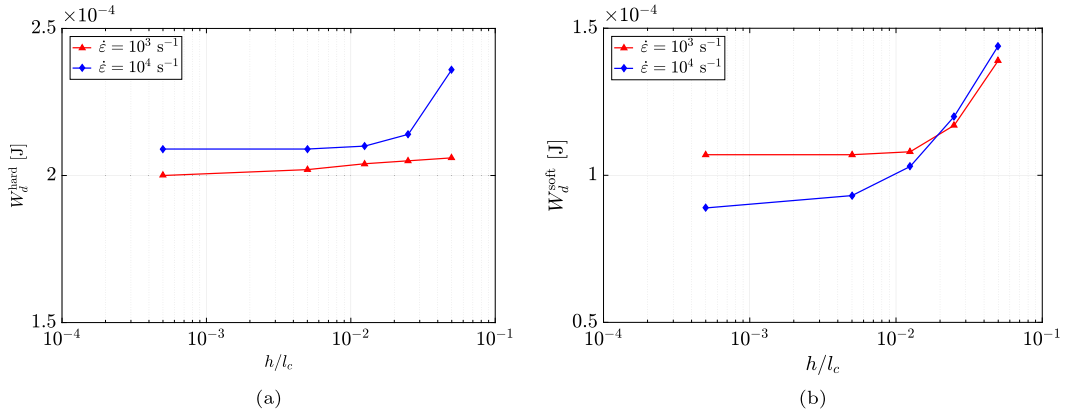


**Figure 8.** Dissipated energy in the hardening (a) and softening (b) zones as a function of the mesh size.

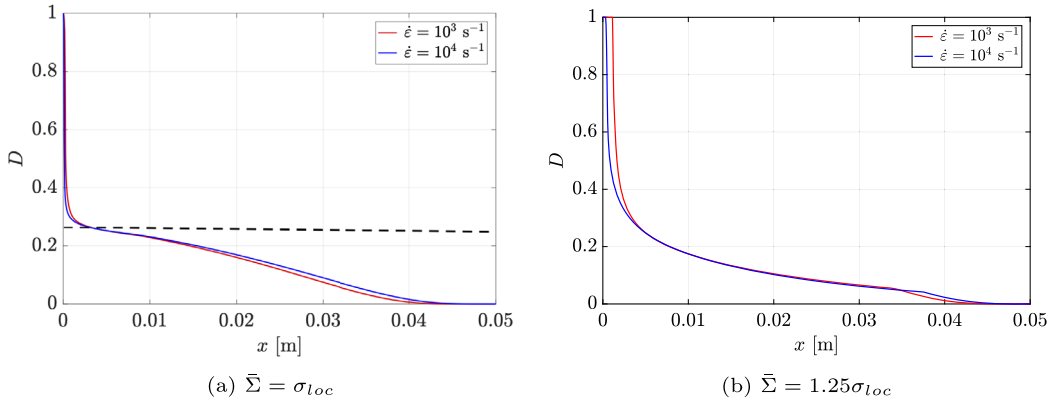


**Figure 9.** Damage profile in the bar at the end of the simulation. The horizontal dotted line corresponds to  $D = D_i$ .

is however harder to get for higher loading rates. This fact may be related to the damage profiles obtained at the end of the simulation and shown in Figure 9(a). The damage gradient is extremely steep and gets steeper for a higher loading rate.

### 5. Third scenario: sudden loading at one extremity of a bar

The bar is now loaded only at its right extremity with a given velocity  $\bar{v}$ . Initial and boundary conditions are given by

$$u(x, t = 0) = 0, \quad \dot{u}(x, t = 0) = 0, \quad D(x, t = 0) = 0 \tag{17}$$

$$\sigma(x = 0, t) = 0, \quad u(x = L, t) = \bar{v}t. \tag{18}$$

This problem was studied for a time-independent model in [20, 24]. These papers give analytical informations on the solution. In particular, it gives the imposed velocity needed to break the material at the extremity. We shall call this velocity localizing velocity  $v_{loc}$ . It is given by

$$v_{loc} = \int_0^{\epsilon_i} c(\epsilon) d\epsilon \tag{19}$$

where  $c(\epsilon)$  is the wave speed for a strain  $\epsilon$  and  $T(\epsilon)$  the tangent to the stress–strain curve:

$$c(\epsilon) = \sqrt{\frac{T(\epsilon)}{\rho}}, \quad T(\epsilon) = \frac{d\sigma}{d\epsilon}. \tag{20}$$

When applied to the time-independent limit case of the delayed damage model (curve  $0^+$  in Figure 1), we get

$$v_{loc} = c_0\epsilon_0 + \int_{\epsilon_0}^{\epsilon_i} c(\epsilon) d\epsilon = c_0\epsilon_0 + c_0 \int_{\epsilon_0}^{\epsilon_i} \left(\frac{2(\epsilon_i - \epsilon)}{\epsilon_c}\right)^{1/2} d\epsilon = c_0 \left(\epsilon_0 + \frac{\epsilon_c}{3}(1 - \epsilon_0/\epsilon_c)^{3/2}\right). \tag{21}$$

We observe numerically with the delayed damage model that the above velocity is the minimal velocity to reach  $D = 1$  at the extremity of the bar. We also note that with the above velocity  $l_1$  is restricted to the last element. Only one element reaches  $D = 1$ . Next to this element, the damage gradient is very steep.

We now analyze whether or not there is a relationship between  $\sigma_{loc}$  observed in the second scenario and  $v_{loc}$ . In the second scenario, the stress wave yields a velocity step of  $\sigma_{loc}/(\rho c_0)$  when the wave reflects. Using the numerically observed value  $\sigma_{loc} = 1.3\sigma_0$ , we get a velocity step of 8.6 m/s which is very close to the 8.5 m/s given in (21).

### 6. Conclusions and discussion

The delayed damage model is an appealing approach to avoid spurious localization in damage analysis leading to failure. Indeed, its introduction in simulation tool is restricted to the constitutive model. The goal of this paper was to analyse whether or not the model was keeping its promises on three different loading scenarii.

For the first scenario, sudden dynamic failure from rest, the delayed damage model fails to regularize. The damage only evolves in a single element during failure and as a consequence, the energy needed for failure goes to zero as the mesh size goes to zero. One may argue that delayed damage model was designed for situations involving a fair amount of kinetic energy and that the observed spurious localization for the first scenario is not an issue in practice. We believe that caution is in order. Indeed, as dissipation occurs, a high level of kinetic energy might eventually yield to situation close to rest in which unwanted further failure with zero dissipation might occur. A final note on the first scenario is that even though damage time derivative is controlled by the delayed damage model, the space derivative is not controlled.

For the second scenario, our findings show that there exist a minimal stress, loading rate independent, to break the bar. For this minimal loading, a single element reaches failure. There is however no spurious localization per se because the dissipated energy (even the softening part) tends to stabilize with the mesh size. This stabilization requires however a very fine mesh since the damage gradient is very high. The fact that the minimal stress needed for failure is independent of the loading rate is an issue since in general the load to failure is observed experimentally as growing with the loading rate. Another thing that needs to be confronted to experiments is that the delayed damage model predicts (for higher loading than the localization stress) a finite size of the fully damaged zone (meaning in practice that a part of the bar turns into powder).

For the third scenario, impact case, the minimal imposed velocity needed for failure was obtained numerically and turns out to be given by the von Karman formula. This formula uses the time-independent part of the model. In other words the obtained limit load does not depend on the  $a$  and  $\tau_c$  parameter of the delayed damage model. Finally, the limit load of the third scenario was connected to the one of the second scenario. We thus conjecture that the localization stress of the second scenario may be obtained for any hardening functions  $f$  by evaluating the localization velocity with the von Karman formula and multiplying the result par  $\rho c_0$ .

This paper is dedicated to the delayed damage models. As recalled in the introduction it is neither the only and nor the first model which has introduced a rate dependent effect for damage. The delayed damage model has however a specificity that the damage rate is bounded. A legitimate question is to ask how other types of rate-damage models would perform for the three scenarii. A commonly used rate damage model is the power law model given below in our simple one-dimensional setting, [16]. Relation (1) is replaced by

$$\dot{D} = \frac{1}{\tau_c} \langle af(Y, D) \rangle_+^n \quad (22)$$

where  $n$  is some positive coefficient and  $D$  is still restricted not to go beyond one. In the above, the damage rate is no longer bounded.

Using  $n = 1$ , and the same parameter as for the delayed damage model for the other parameter, we carried out the three scenarii with the power-law model. For the first scenario results did not change, ie spurious localization in a single element. Regarding the second scenario, the localization stress and the damage profile for  $D > D_i$  are not affected. Finally, the localization velocity for the third scenario is not modified either. The fact that the localization velocity and stress are the same for delayed damage and power law model are not surprising since they are linked only to the expression of  $f$  (that is the rate-independent part of the model) and not to the specifics of the rate-dependency of the model.

A natural next step to this work is to analyze softening visco-plastic models and check their robustness with regards to the three scenarii.

## References

- [1] O. Allix, J.-F. Deü, "Delayed-damage modelling for fracture prediction of laminated composites under dynamic loading", *Eng. Trans.* **45** (1997), no. 1, p. 29-46.
- [2] Z. P. Bazant, T. Belytschko, "Wave propagation in a strain-softening bar: exact solution", *J. Eng. Mech.* **111** (1985), p. 381-389.
- [3] G. Pijaudier-Cabot, Z. P. Bazant, M. Tabbara, "Comparison of various models for strain softening", *Eng. Comput.* **5** (1988), p. 141-150.
- [4] Z. P. Bazant, T. Belytschko, T.-P. Chang, "Continuum theory for strain-softening", *J. Eng. Mech.* **110** (1984), p. 1666-1692.
- [5] G. Pijaudier-Cabot, Z. P. Bazant, "Nonlocal damage theory", *J. Eng. Mech. ASCE* **113** (1987), p. 1512-1533.
- [6] H. L. Schreyer, Z. Chen, "One-dimensional softening with localization", *J. Appl. Mech.* **53** (1986), p. 791-797.
- [7] N. Triantafyllidis, E. Aifantis, "A gradient approach to localization of deformation. I. Hyperelastic materials", *J. Elast.* **16** (1986), p. 225-237.
- [8] M. Frémond, B. Nedjar, "Damage, gradient of damage and principle of virtual power", *Int. J. Solids Struct.* **33** (1996), no. 8, p. 1083-1103.
- [9] R. Peerlings, R. De Borst, W. A. M. Brekelmans, J. Vree, "Gradient-enhanced damage for quasi-brittle materials", *Int. J. Numer. Methods Eng.* **39** (1996), p. 3391-3403.
- [10] G. Pijaudier-Cabot, N. Burlion, "Damage and localisation in elastic materials with voids", *Mech. Cohesive Frict. Mater.* **144** (1996), p. 129-144.
- [11] V. Hakim, A. Karma, "Laws of crack motion and phase-field models of fracture", *J. Mech. Phys. Solids* **57** (2009), no. 2, p. 342-368.
- [12] B. Bourdin, G. a. Francfort, J.-J. Marigo, "The variational approach to fracture", *J. Elast.* **91** (2008), p. 5-148.
- [13] N. Moës, C. Stolz, P.-E. Bernard, N. Chevaugeon, "A level set based model for damage growth: the thick level set approach", *Int. J. Numer. Methods Eng.* **86** (2011), no. 3, p. 358-380.
- [14] R. Becker, A. Needleman, O. Richmond, V. Tvergaard, "Void growth and failure in notched bars", *J. Mech. Phys. Solids* **36** (1988), no. 3, p. 317-351.
- [15] L. J. Sluys, "Wave propagation, localisation and dispersion in softening solids", PhD Thesis, T.U. Delft, 1992.
- [16] J. C. Simo, J. W. Ju, "Strain- and stress-based continuum damage models. I. formulation", *Int. J. Solids Struct.* **23** (1987), p. 821-840.
- [17] J.-F. Dubé, G. Pijaudier-Cabot, C. L. Borderie, "Rate dependent damage model for concrete in dynamics", *J. Eng. Mech.* **122** (1996), no. 10, p. 939-947.
- [18] P. Perzyna, "Fundamental problems in viscoplasticity", *Adv. Appl. Mech.* **9** (1966), p. 243-377.

- [19] O. Allix, J. F. Deü, P. Ladevèze, “A delay damage meso-model for prediction of localisation and fracture of laminates subjected to high rates loading”, in *Proceedings, European Conference on Computational Mechanics, München, Germany*, Wiley, 1999.
- [20] T. von Karman, “On the propagation of plastic deformation in solids”, Tech. Report OSRD 365, NDRC Report No A-29, 1942.
- [21] T. Belytschko, L. Wing-Kam, K. Moran, B. Elkhodary, *Nonlinear Finite Elements for Continua and Structures*, 2nd ed., Wiley, UK, 2013.
- [22] A. Suffis, T. Lubrecht, A. Combescure, “Damage model with delay effect: Analytical and numerical studies of the evolution of the characteristic damage length”, *Int. J. Solids Struct.* **40** (2003), no. 13–14, p. 3463-3476.
- [23] A. Suffis, A. Combescure, “Modèle d’endommagement à effet retard: Etude numérique et analytique de l’évolution de la longueur caractéristique”, *Revu. Euro. Eléments* **11** (2002), no. 5, p. 593-619.
- [24] T. Von Karman, P. Duwez, “The propagation of plastic deformation in solids”, *J. Appl. Phys.* **21** (1950), no. 10, p. 987-994.